Chapter 6: Actuators and Sensors, Motors and Generators

6.1 Force-induced electric and magnetic fields

6.1.1 Introduction

Chapter 5 explained how electric and magnetic fields could exert force on charges, currents, and media, and how electrical power into such devices could be transformed into mechanical power. Chapter 6 explores several types of practical motors and actuators built using these principles, where an actuator is typically a motor that throws a switch or performs some other brief task from time to time. Chapter 6 also explores the reverse transformation, where mechanical motion alters electric or magnetic fields and converts mechanical to electrical power. Absent losses, conversions to electrical power can be nearly perfect and find application in electrical generators and mechanical sensors.

Section 6.1.2 first explores how mechanical motion of conductors or charges through magnetic fields can generate voltages that can be tapped for power. Two charged objects can also be forcefully separated, lengthening the electric field lines connecting them and thereby increasing their voltage difference, where this increased voltage can be tapped for purposes of sensing or electrical power generation. Section 6.1.3 then shows in the context of a current-carrying wire in a magnetic field how power conversion can occur in either direction.

6.1.2 Motion-induced voltages

Any conductor moving across magnetic field lines acquires an open-circuit voltage that follows directly from the Lorentz force law (6.1.1)[18]:

$$\bar{f} = q(\bar{E} + \bar{v} \times \mu_o \bar{H}) \tag{6.1.1}$$

Consider the electron illustrated in Figure 6.1.1, which has charge –e and velocity $\bar{v}$.

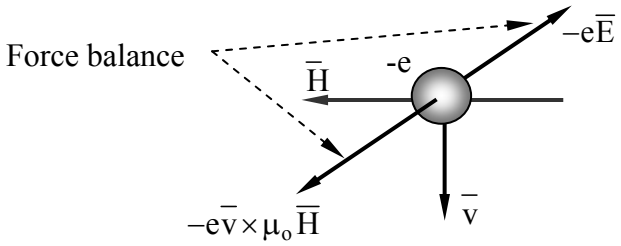

Figure 6.1.1 Forces on an electron moving through electromagnetic fields.

[18] Some textbooks present alternative explanations that lead to the same results. The explanation here views matter as composed of charged particles governed electromagnetically solely by the Lorentz force law, and other forces, such as the Kelvin force densities acting on media discussed in Section 4.5, are derived from it.

It is moving perpendicular to $\bar{H}$ and therefore experiences a Lorentz force on it of $-e\bar{v}\times\mu_o\bar{H}$. It experiences that force even inside a moving wire and will accelerate in response to it. This force causes all free electrons inside the conductor to move until the resulting surface charges produce an equilibrium electric field distribution such that the net force on any electron is zero.

In the case of a moving open-circuited wire, the free charges (electrons) will move inside the wire and accumulate toward its ends until there is sufficient electric potential across the wire to halt their movement everywhere. Specifically, this Lorentz force balance requires that the force $-e\bar{E}_e$ on the electrons due to the resulting electric field $\bar{E}_e$ be equal and opposite to those due to the magnetic field $-e\bar{v}\times\mu_o\bar{H}$, that is:

$$-e\bar{v}\times\mu_o\bar{H} = e\bar{E}_e \tag{6.1.2}$$

Therefore the equilibrium electric field inside the wire must be:

$$\bar{E}_e = -\bar{v}\times\mu_o\bar{H} \tag{6.1.3}$$

There should be no confusion about $\bar{E}_e$ being non-zero inside a conductor. It is the net force on free electrons that must be zero in equilibrium, not the electric field $\bar{E}_e$. The electric Lorentz force $q\bar{E}_e$ must balance the magnetic Lorentz force or otherwise the charges will experience a net force that continues to move them until there is such balance.

Figure 6.1.2 illustrates such a wire of length W moving at velocity $\bar{v}$ perpendicular to $\bar{H}$.

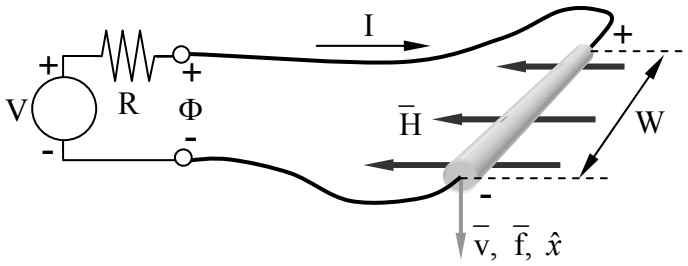

Figure 6.1.2 Forces and voltages on a wire moving in a magnetic field.

If the wire were open-circuited, the potential Φ across it would be the integral of the electric field necessary to cancel the magnetic forces on the electrons, where:

$$\Phi = v\mu_o HW \tag{6.1.4}$$

and the signs and directions are as indicated in the figure. We assume that the fields, wires, and velocity $\bar{v}$ in the figure are all orthogonal so that $\bar{v}\times\mu_o\bar{H}$ contributes no potential differences except along the wire of length W.

Example 6.1A

A large metal airplane flies at 300 m s^{-1} relative to a vertical terrestrial magnetic field of ~10^{-4} Teslas (1 gauss). What is the open-circuit voltage V wingtip to wingtip if the wingspan W is ~40 meters? If $\overline{B}$ points upwards, is the right wing positive or negative?

Solution: The electric field induced inside the metal is $-\overline{v}\times\mu_o\overline{H}$ (4.3.2), so the induced voltage $V = Wv\mu_oH \cong 40\times300\times1.26\times10^{-6}\times10^{-4} \cong 1.5\times10^{-6}$ volts, and the right wingtip is positive.

6.1.3 Induced currents and back voltages

If the moving wire of Figure 6.1.2 is connected to a load R, then current I will flow as governed by Ohm's law. I depends on Φ, R, and the illustrated Thevenin voltage V:

$$I = (V-\Phi)/R = \left(V - v\mu_o HW\right)/R \tag{6.1.5}$$

The current can be positive or negative, depending on the relative values of V and the motion-induced voltage Φ. From (5.2.7) we see that the magnetic force density on the wire is $\overline{F} = \overline{I}\times\mu_o\overline{H}$ [Nm^{-1}]. The associated total force $\overline{f}_{be}$ exerted on the wire by the environment and by $\overline{H}$ follows from (6.1.5) and is:

$$\overline{f}_{be} = \overline{I}\times\mu_o\overline{H}W = \hat{x}\mu_o HW(V-\Phi)/R \quad [N] \tag{6.1.6}$$

where the unit vector $\hat{x}$ is parallel to $\overline{v}$.

Equation (6.1.6) enables us to compute the mechanical power delivered to the wire by the environment (P_{be}) or, in the reverse direction, by the wire to the environment (P_{oe}), where $P_{be} = -P_{oe}$. If the voltage source V is sufficiently great, then the system functions as a motor and the mechanical power P_{oe} delivered to the environment by the wire is:

$$P_{oe} = \overline{f}_{oe}\bullet\overline{v} = v\mu_o HW(V-\Phi)/R = \Phi(V-\Phi)/R \quad [W] \tag{6.1.7}$$

The electrical power P_e delivered by the moving wire to the battery and resistor equals the mechanical power P_{be} delivered to the wire by the environment, where I is given by (6.1.5):

$$\begin{aligned} P_e &= -VI + I^2R = -\left[V(V-\Phi)/R\right] + \left[(V-\Phi)^2/R\right] = \left[(V-\Phi)/R\right]\left[-V+(V-\Phi)\right] \\ &= -\Phi(V-\Phi)/R = P_{be} \quad [W] \end{aligned} \tag{6.1.8}$$

The negative sign in the first term of (6.1.8) is associated with the direction of I defined in Figure 6.1.2; I flows out of the Thevenin circuit while P_e flows in. If V is zero, then the wire delivers maximum power, Φ^2/R. As V increases, this delivered power diminishes and then becomes negative as the system ceases to be an electrical generator and becomes a motor. As a motor the

mechanical power delivered to the wire by the environment becomes negative, and the electrical power delivered by the Thevenin source becomes positive. That is, we have a:

Motor: If mechanical power out $P_{oe} > 0$,
$V > \Phi = v\mu_o HW$, or $v < V/\mu_o HW$ (6.1.9)

Generator: If electrical power out $P_e > 0$,
$V < \Phi$, or $v > V/\mu_o HW$ (6.1.10)

We call Φ the "*back voltage*" of a motor; it increases as the motor velocity v increases until it equals the voltage V of the power source and $P_e = 0$. If the velocity increases further so that $\Phi > V$, the motor becomes a generator. When $V = \Phi$, then $I = 0$ and the motor moves freely without any electromagnetic forces.

This basic coupling mechanism between magnetic and mechanical forces and powers can be utilized in many configurations, as discussed further below.

Example 6.1B

A straight wire is drawn at velocity $\bar{v} = \hat{x}\, 10$ m s^{-1} between the poles of a 0.1-Tesla magnet; the velocity vector, wire direction, and field direction are all orthogonal to each other. The wire is externally connected to a resistor $R = 10^{-5}$ ohms. What mechanical force $\bar{f}$ is exerted on the wire by the magnetic field $\bar{B}$? The geometry is illustrated in Figure 6.1.2.

Solution: The force exerted on the wire by its magnetic environment (6.1.6) is
$\bar{f}_{be} = \bar{I} \times \bar{H}\mu_o W$ [N], where the induced current $I = -\Phi/R$ and the back voltage $\Phi = v\mu_o HW$ [V]. Therefore:
$f_{be} = -\hat{x}\, \mu_o HW\Phi/R = -\hat{x}\, v(\mu_o HW)^2/R = -\hat{x}\, 10\times(0.1\times0.1)^2/10^{-5} = 1$ [N], opposite to $\bar{v}$.

6.2 Electrostatic actuators and motors

6.2.1 Introduction to Micro-Electromechanical Systems (MEMS)

Chapter 6 elaborates on Chapter 5 by exploring a variety of motors, generators, and sensors in both linear and rotary configurations. Electric examples are analyzed in Section 6.2, and magnetic examples in Section 6.3. Section 6.2.1 reviews the background, while Sections 6.2.2 and 6.2.3 explore parallel-capacitor-plate devices using linear and rotary motion respectively. Section 6.2.4 discusses electrostatic motors exerting forces on dielectrics, while Section 6.2.5 discusses the limits to power density posed by electrical breakdown of air or other media, which limits peak electric field strength.

Micro-electromechanical systems (MEMS) are commonly used as motors, generators, actuators, and sensors and underlie one of the major current revolutions in electrical engineering, namely the extension of integrated circuit fabrication technology to electromechanical systems on the same substrate as the circuits with which they interoperate. Such devices now function as

optical switches, radio-frequency switches, microphones, accelerometers, thermometers, pressure sensors, chemical sensors, micro-fluidic systems, electrostatic and magnetic motors, biological sensors, and other devices. They are used in systems as diverse as video projectors, automobile air bag triggers, and mechanical digital memories for hot environments.

Advantages of MEMS over their larger counterparts include size, weight, power consumption, and cost, and also much increased speed due to the extremely small masses and distances involved. For example, some MEMS electromechanical switches can operate at MHz frequencies, compared to typical speeds below ~1 kHz for most traditional mechanical devices. The feature size of MEMS ranges from sub-microns or microns up to one or more millimeters, although the basic electromagnetic principles apply to devices of any scale. Recent advances in micro-fabrication techniques, such as new lithography and etching techniques, precision micro-molds, and improved laser cutting and chipping tools, have simplified MEMS development and extended their capabilities.

The *Lorentz force law* (6.2.1) is fundamental to all electric and magnetic motors and generators and expresses the force vector $\bar{f}$ [Newtons] acting on a charge q [Coulombs] as a function of the local electric field $\bar{E}$, magnetic field $\bar{H}$, and charge velocity vector $\bar{v}$ [ms^{-1}]:

$$\bar{f} = q\left(\bar{E} + \bar{v} \times \mu_o \bar{H}\right) \quad \text{[Newtons]} \tag{6.2.1}$$

For the examples in Section 6.2 the velocities $\bar{v}$ and magnetic fields $\bar{H}$ are negligible, so the force is primarily electrostatic, $\bar{f} = q\bar{E}$, and can be readily found if $\bar{E}$ is known. When $\bar{E}$ is unknown, the energy method of Section 5.4.2 can often be used instead, as illustrated later. The power densities achievable in MEMS devices can be quite high, and are typically limited by materials failures, such as electrical breakdown or ohmic overheating.

6.2.2 Electrostatic actuators

The simplest MEMS actuators use the electric force between two capacitor plates to pull them together, as illustrated in Figure 6.2.1(a) for a cantilevered loudspeaker or switch. The Lorentz force density F [N m^{-2}] attracting the two plates is given by the $q\bar{E}$ term in (6.2.1). Although one might suppose the force density on the upper plate is simply $\rho_s E$, where ρ_s is the surface charge density [C m^{-2}] on that plate, the correct force is half this value because those charges nearer the surface screen those behind, as suggested in Figure 6.2.1(b); the charges furthest from the surface perceive almost no $\bar{E}$ at all. The figure shows a one-to-one correspondence between electric field lines and charges in a highly idealized distribution—reality is more random. The figure shows that the average field strength E perceived by the charges is half the surface field E_o, independent of their depth distribution $\rho(z)$. Therefore the total attractive electric pressure is:

$$P_e = \rho_s \left(E_o/2\right) \left[\mathrm{Nm}^{-2}\right] \tag{6.2.2}$$

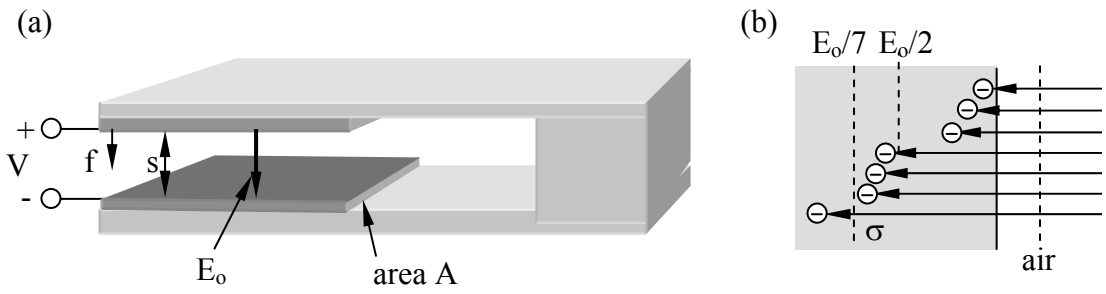

Figure 6.2.1 Electrostatic MEMS switch and forces on a charged conductor.

But the boundary condition at a conductor (2.6.15) is $\hat{n} \bullet \overline{D} = \rho_s$, so:

$$\rho_s = \varepsilon_o E_o \tag{6.2.3}$$

$$P_e = \varepsilon_o E_o^{\,2}/2 \ \left[\mathrm{Nm}^{-2}\right] \quad (\textit{electric pressure} \text{ attracting capacitor plate}) \tag{6.2.4}$$

This is the same pressure derived more rigorously in (5.2.4) and (5.4.3).

If E_o is near its breakdown value $E_B \cong 10^8$ [V m^{-1}] for gaps less than ~10^{-6} meters, then the pressure $P = \varepsilon_o E_o^{\,2}/2 \cong 8.8\times10^{-12}\times10^{16}/2 = 4.4\times10^4$ [N m^{-2}]. A *Newton* is approximately the gravitational force on the apple that fell on Newton's head (prompting his theory of gravity), or on a quarter-pound of butter. Therefore this maximum electrostatic force density is about one pound per square centimeter, comparable to that of a strong magnet.

The cantilever acts like a spring with a *spring constant* k, so the total force f is simply related to the deflection x: f = kx = PA, where A is the area of the capacitor plate. Thus the deflection is:

$$x = PA/k = \varepsilon_o E_o^{\,2} A/2k \ \ [\mathrm{m}] \tag{6.2.5}$$

The ratio A/k is controlled by the composition, thickness, and length of the cantilever, and the desired deflection is controlled by the application. For example, k must be adequate to overcome stiction[19] in switches that make and break contact, and x must be adequate to ensure that the voltage between the capacitor plates does not cause arcing when the switch is open.

Alternatively both capacitor plates could be charged positive or negative so they repel each other. In this case the charge Q moves to the outside surfaces and connects to the very same field strengths as before due to boundary conditions ($E = Q/\varepsilon_o A$) , except that the negative pressure $\varepsilon_o E^2/2$ on the two plates acts to pull them apart rather than together. The field between the plates is then zero.

[19] Stiction is the force that must be overcome when separating two contacting surfaces. These forces often become important for micron-sized objects, particularly for good conductors in contact for long periods.

Even with extreme electric field strengths the power density [W m^{-3}] available with linear motion MEMS actuators may be insufficient. Power equals force times velocity, and rotary velocities can be much greater than linear velocities in systems with limited stroke, such as the cantilever of Figure 6.2.1(a) or the lateral-displacement systems illustrated in Figure 6.2.2. Since it is difficult to compute the lateral electric fields responsible for the lateral forces in rotary or linear systems [e.g., the z components in Figure 6.2.2(a)], the energy methods described below are generally used instead.

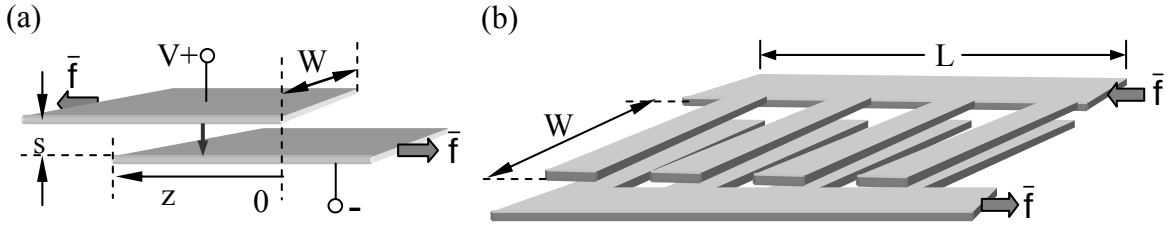

Figure 6.2.2 Electrostatic actuators comprising partially overlapping capacitor plates.

The two charged parallel plates illustrated in Figure 6.2.2(a) are pulled laterally toward one another (z increases) because opposite charges attract. The force $\bar{f}$ required to pull the plates apart depends only on their electric charge q and the plate geometry, independent of any attached circuit. This force $\bar{f}$ in the -z direction can be found by noting that f does work on the capacitor/circuit system, increasing its total energy w_T if f is positive:

$$f = - dw_T/dz = - dw_e/dz - V\, dq/dz \;\; [N] \qquad \text{(energy-force equation)} \qquad (6.2.6)$$

where w_e is the electric energy stored in the capacitor, V is the capacitor voltage[20], and dq is incremental charge flowing from any attached circuit into the positive terminal of the capacitor. The negative sign in (6.2.6) results because f is in the -z direction. Since this energy-force equation is correct regardless of any attached circuit, we can evaluate it for an attached open circuit, battery, or arbitrary Thevenin equivalent, provided it results in the given capacitor voltage V and charge q.

The force computed using (6.2.6) is the same for any attached circuit and any form of the energy expression (3.1.16):

$$w_e = CV^2/2 = q^2/2C \;\; [J] \qquad \text{(electric energy in a capacitor)} \qquad (6.2.7)$$

The algebra is minimized, however, if we assume the capacitor is open-circuit so that q is constant and dq/dz = 0 in (6.2.6). Because V depends on z in this case, it is simpler to use $w_e = q^2/2C$ to evaluate (6.2.6), where: 1) $C = \varepsilon_o Wz/s$ [F], 2) the overlap area of the capacitor is Wz, 3) the plate separation is s << W, and 4) we neglect fringing fields. Thus (6.2.6) becomes:

$$f = - (q^2/2)\,(dC^{-1}/dz) = - (q^2/2)(s/\varepsilon_o W)dz^{-1}/dz = (q^2/2)(s/\varepsilon_o Wz^2) \;\; [N] \qquad (6.2.8)$$

[20] For convenience, V represents voltage and v represents velocity in this section.

The rapid increase in force as $z \to 0$ results because q is constant and concentrates at the ends of the plates as the overlap approaches zero; $z \to 0$ also violates the assumption that fringing fields can be neglected.

It is interesting to relate the force f of (6.2.8) to the electric field strength E, where:

$$E = \rho_s/\varepsilon_o = q/Wz\varepsilon_o \ \ [V\ m^{-1}] \tag{6.2.9}$$

$$q = Wz\varepsilon_o E = Wz\varepsilon_o V/s \ \ [C] \tag{6.2.10}$$

$$f = q^2 s/2\varepsilon_o W z^2 = Ws\varepsilon_o E^2/2 = A'P_e \ \ [N] \qquad \text{(lateral electric force)} \tag{6.2.11}$$

where A' = Ws is the cross-sectional area of the gap perpendicular to $\bar{f}$, and $P_e = \Delta W_e = \varepsilon_o E^2/2 - 0$ is the electric pressure difference acting at the end of the capacitor. Note that this pressure is perpendicular to $\bar{E}$ and is "pushing" into the adjacent field-free region where $W_e = 0$; in contrast, the pressure parallel to $\bar{E}$ always "pulls". Later we shall find that "magnetic pressure" $P_m = \Delta W_m$ is similarly attractive parallel to $\bar{H}$ and pushes in directions orthogonal to $\bar{H}$.

Note that if V is constant, then the force f (6.2.11) does not depend on z and is maximized as $s \to 0$. For a fixed V, the minimum practical plate separation s corresponds to E near the threshold of electrical breakdown, which is discussed further in Section 6.2.5. Also note that the force f is proportional to W, which can be maximized using multiple fingers similar to those illustrated in Figure 6.2.2(b). Actuator and motor designs generally maximize f and W while preserving the desired stroke[21].

Example 6.2A

Design a small electrostatic overlapping plate linear actuator that opens a latch by moving 1 mm with a force of 10^{-2} Newtons.

Solution: The two-plate actuator illustrated in Figure 6.2.2(a) exerts a force $f = Ws\varepsilon_o E^2$ (6.2.11). If E is near the maximum dry-gas value of $\sim 3.2\times10^6$ V m^{-1}, the gap s = 1 mm, and W = 1 cm, then $f = 10^{-2}\times10^{-3}\times8.85\times10^{-12}\times10^{13} = 8.85\times10^{-4}$ [N]. By using M fingers, each wider than the 1-mm stroke, the force can be increased by M [see Figure 6.2.2(b)]. If we let M = 12 the device yields $f = 1.06\times10^{-2}$, but its length L must be greater than 12 times twice the finger width (see figure), where the finger width G must exceed not only the stroke but also several times s, in order to make fringing fields negligible. If $G \cong 4$ mm, then the actuator length is $12\times2\times4$ mm = 9.6 cm, large compared to the width. A three-plate actuator with two grounded plates on the outside and one charged plate inside would double the force, halve the length L, protect users from electrocution, and simplify sealing the actuator against moisture

[21] The "stroke" of an actuator is its range of positions; in Figure 6.2.2(a) it would be the maximum minus the minimum value of z. Although the force (6.2.11) becomes infinite as the minimum $z \to 0$ for constant q, this would violate the assumption $z >> d$ and can cause $V \to \infty$; V is usually held constant, however.

that could short-circuit the plates. The plate voltage V = Es = 3200 volts. This design is not unique, of course.

6.2.3 Rotary electrostatic motors

Because forces (6.2.4) or (6.2.11) in electrostatic motors are limited by the maximum electric field strength E possible without electric arcing, higher power densities [W m^{-3}] require higher speeds since the power P = fv [watts], where f is force [N], and v is velocity [m s^{-1}]. Figure 6.2.3 pictures an ideal 4-segment rotary *electrostatic motor* for which v and the resulting centrifugal forces are ultimately limited by the tensile strength of the rotor. For both materials and aerodynamic reasons the maximum v at the rotor tip is usually somewhat less than the speed of sound, ~340 m/s. Some rotors spin much faster in vacuum if the material can withstand the centrifugal force.

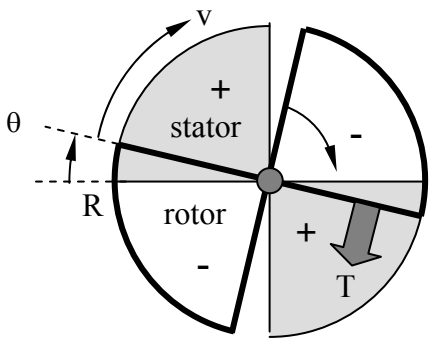

Figure 6.2.3 Four-segment rotary electrostatic motor.

This motor has radius R, plate separation s, and operating voltage V. Stationary "*stator*" plates occupy two quadrants of the motor and a second pair of quadrant plates (the "*rotor*") can rotate to yield an overlap area $A = R^2\theta$ [m^2] that varies from zero to $\pi R^2/2$ as θ increases from zero to π/2. If the voltage V is applied across the plates, a *torque* T is produced[22], where:

$$T = -dw_T/d\theta \ \ [\text{N m}] \tag{6.2.12}$$

and dw_T is the increment by which the total system energy (fields plus battery) is <u>increased</u> as a result of the motion dθ. The negative sign in (6.2.12) reflects the fact that the torque T is applied by the motor to the environment. If we replace the overlap area of Wz in (6.2.8) by its equivalent $R^2\theta$, then (6.2.8) and (6.2.12) become:

$$w_e = Q^2/2C = Q^2 s/2\varepsilon_o R^2\theta \tag{6.2.13}$$

[22] Torque T [Nm] equals the force f on a lever times its length L. Therefore the mechanical work performed by the torque is $w_m = fx = fL(x/L) = T\theta$, where $\theta = x/L$ is the angle (radians) through which the lever rotates about its pivot at one end. Power is $Td\theta/dt = T\omega$ [W].

$$T = -dw_T/d\theta = Q^2 s/2\varepsilon_o R^2\theta^2 = \varepsilon_o R^2 V^2/s \ \ [\text{N m}] \tag{6.2.14}$$

where $Q = \varepsilon_o R^2\theta V/s$ [C], which follows from (6.2.10) where $Wz \rightarrow R^2\theta$ [m^2].

If we assume $R = 10^{-3}$, $s = 10^{-6}$, and $V = 3$ volts (corresponding to 3×10^6 Vm^{-1}, below the breakdown limit discussed in Section 6.2.5; then (6.2.14) yields:

$$T = 8.8\times10^{-12}\times(10^{-3})^2 3^2/10^{-6} \cong 7.9\times10^{-11} \ \ [\text{N m}] \tag{6.2.15}$$

This torque exists only until the plates fully overlap, at which time the voltage V is switched to zero until the plates coast another 90° and V is restored. The duty cycle of this motor is thus 0.5 because $T \neq 0$ only half of the time.

A single such ideal motor can then deliver an average of $T\omega/2$ watts, where the factor ½ reflects the duty cycle, and $T\omega$ is the mechanical power associated with torque T on a shaft rotating at ω radians s^{-1}. If the tip velocity v of this rotor is 300 ms^{-1}, slightly less than the speed of sound so as to reduce drag losses while maximizing ω, then the corresponding angular velocity ω is $v/R = 300/10^{-3} = 3\times10^5$ radians s^{-1} or $\sim3\times10^6$ rpm, and the available power $T\omega/2 \cong 7.9\times10^{-11} \times 3\times10^5/2 \cong 1.2\times10^{-5}$ watts if we neglect all losses. In principle one might pack ~25,000 motors into one cubic centimeter if each motor were 10 microns thick, yielding ~0.3 W/cm^3. By using a motor with N segments instead of 4 this power density and torque could be increased by a factor of N/4. The small micron-sized gap s would permit values of N as high as ~500 before the fringing fields become important, and power densities of ~40 W/cm^{-3}.

This 40-W/cm^3 power density can be compared to that of a 200-hp automobile engine that delivers 200×746 watts[23] and occupies 0.1 m^3, yielding only ~1.5 W/cm^3. Extremely high power densities are practical only in tiny MEMS devices because heat and torque are then easier to remove, and because only micron-scale gaps permit the highest field strengths, as explained in Section 6.2.5. Rotary MEMS motors have great potential for extremely low power applications where torque extraction can be efficient; examples include drivers for micro-gas-turbines and pumps. The field of MEMS motors is still young, so their full potential remains unknown.

6.2.4 Dielectric actuators and motors

One difficulty with the rotary motor of Figure 6.2.3 is that voltage must be applied to the moving vanes across a sliding mechanical boundary. One alternative is to use a dielectric rotor driven by voltages applied only to the stator. The configuration could be similar to that of Figure 6.2.3 but the rotor would be dielectric and mounted between identical conducting stators with a potential V between them that is turned on and off at times so as to produce an average torque as the rotor rotates. Figure 6.2.4 illustrates the concept in terms of a linear actuator for which the force f can more easily be found. We again assume that fringing fields can be neglected because $W >> d$.

[23] There are 746 watts per horsepower.

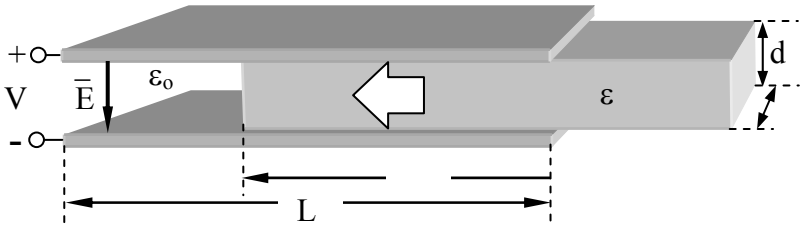

Figure 6.2.4 Linear dielectric slab actuator.

The force f can be found by differentiating the total stored electric energy w_e with respect to motion z, where C is the effective capacitance of this structure, and:

$$w_e = CV^2/2 = Q^2/2C \ \ [J] \tag{6.2.16}$$

To simplify differentiating w_e with respect to z, it is easier to use the expression $w_e = Q^2/2C$ because is this case Q is independent of z whereas C is not.

For two capacitors in parallel $C = C_o + C_\varepsilon$ (3.1.14), where C_o and C_ε are the capacitances associated with the air and dielectric halves of the actuator, respectively. Capacitance C was defined in (3.1.8), and equals εA/s where A is the plate area and s is the plate separation. It follows that:

$$C = C_\varepsilon + C_o = \varepsilon zW/s + \varepsilon_o(L - z)W/s = [z(\varepsilon - \varepsilon_o) + \varepsilon_o L]W/s \tag{6.2.17}$$

The force f pulling the dielectric slab between the charged plates is given by the force-energy relation (6.2.6) and can be combined with (6.2.16) and (6.2.17) to yield:

$$\begin{aligned} f \cong -dw_e/dz &= -d\left(Q^2/2C\right)/dz = -\left(Q^2 s/2W\right) d\left[z(\varepsilon-\varepsilon_o)+\varepsilon_o L\right]^{-1}/dz \\ &= \left(Q^2 s/2W\right)\left[z(\varepsilon-\varepsilon_o)+\varepsilon_o L\right]^{-2}(\varepsilon-\varepsilon_o) = \left(Q^2 W/2sC^2\right)(\varepsilon-\varepsilon_o)\,[N] \end{aligned} \tag{6.2.18}$$

This force can be expressed in terms of the electric field strength E between the two plates by substituting into (6.2.18) the expressions Q = CV and V = Es:

$$f \cong (E^2 sW/2)(\varepsilon - \varepsilon_o) = [(\varepsilon - \varepsilon_o)E^2/2]Ws = \Delta P_e A \ [N] \tag{6.2.19}$$

where A = Ws is the area of the endface of the dielectric slab, and the differential electric pressure pulling the slab between the charged plates is:

$$\Delta P_e = (\varepsilon - \varepsilon_o)E^2/2 \ \ [Nm^{-2}] \tag{6.2.20}$$

The differential pressure ΔP_e pushing the interface into the capacitor is thus the difference between the electric pressure on one side of the dielectric interface and that on the other, where the pressure P_e on each side is simply the electric energy density there:

$$P_e = \varepsilon E^2/2 \ \ [Nm^{-2}], [Jm^{-3}] \qquad (6.2.21)$$

Because the electric field at the right-hand end of the slab approaches zero, it exerts no additional force. Electric pressure is discussed further in Section 5.5.2.

Applying these ideas to the rotary motor of Figure 6.2.3 simply involves replacing the rotor by its dielectric equivalent and situating it between conducting stator plates that are excited by V volts so as to pull each dielectric quadrant into the space between them. Then V is switched to zero as the dielectric exits that space so the rotor can coast unpowered until the dielectric quadrants start entering the next pair of stator plates. Thus the drive voltage V is non-zero half the time, with two voltage pulses per revolution of this two-quadrant rotor. The timing of the voltages must be responsive to the exact position of the rotor, which is often determined by a separate rotor angular position sensor. Start-up can fail if the rotor is in exactly the wrong position where f = 0 regardless of V, and the rotor will spin backwards if it starts from the wrong position. Figure 6.3.6 suggests how multiple segments and excitation phases can avoid this problem in the context of magnetic motors.

Example 6.2B

Design a maximum-power-density rotary electrostatic motor that delivers 10 W power at $\omega \cong 10^6$ r s^{-1} without make/break or sliding electrical contacts.

Solution: A segmented dielectric rotor sandwiched between charged conducting plates avoids sliding electrical contacts. Assume the rotor has radius R, thickness s, and is made of two electrically insulated dielectrics having permittivities $\varepsilon = 10\varepsilon_o$ and ε_o, and that they are radially segmented as is the rotor in Figure 6.2.3, but with M segments rather than 4. The maximum pressure on the edges of the rotor dielectric boundaries between ε and ε_o is $\Delta P_e = (\varepsilon - \varepsilon_o)E^2/2$ [N m^{-2}]. The mechanical power delivered during the half cycle the voltages are applied to the plate is $T\omega = 20 = \Delta P_e(R/2)sM\omega$. Let's arbitrarily set $s = 10^{-6}$, $E = 10^6$ [V m^{-1}], and M = 800. Therefore $R = 2\times20/(sM\omega\Delta P_e) = 40/[10^{-6}\times800\times10^6\times9\times8.85\times10^{-12}\times(10^6)^2/2] = 1.3\times10^{-3}$ [m]. The operating voltage is Es ≅ 1 volt and the power density is ~10^5 W/cm^3.

6.2.5 Electrical breakdown

In every case the torque or force produced by an electrostatic MEMS actuator or motor is limited by the *breakdown field* $E_B = V_B/d$, where V_B is the *breakdown voltage*, and the dependence of E_B on d is non-linear. Electric breakdown of a gas occurs when stray free electrons accelerated by E acquire enough velocity and energy (a few electron volts[24]) to knock additional free electrons off gas molecules when they collide, thus triggering a chain reaction that leads to arcing and potentially destructive currents. Water molecules shed electrons much more easily in collisions than do nitrogen or oxygen molecules, and so E_B is much lower in moist air. This is why it is easier to draw visible sparks in cold dry winter air than it is in summer, because in winter the

[24] An electron volt is the energy acquired by an electron or other equally charged particle as it accelerates through a potential difference of one volt. It is equivalent to $e = 1.6021\times10^{-19}$ Joules.

field strengths can be much greater before breakdown occurs, and such high-voltage breakdowns are more visible.

If, however, the gap between the two electrodes is sufficiently small, the probability diminishes that an ionizing collision will occur between any free electron and a gas atom before the electron hits the positively charged electrode. This *mean-free-path,* or average distance before a "collision", for free electrons is on the order of one micron in air, so breakdown is inhibited for gaps less than the mean free path. However, even when the gap is so narrow that gas breakdown is unlikely, if the field strength E is increased to $\sim 3 \times 10^8$ [V m^{-1}], or two orders of magnitude beyond typical values for E_B in dry gas, any free electrons can then acquire enough energy to knock an ion loose from the positively charged wall. Such a positive ion can then acquire enough energy to release multiple electrons when it impacts the negatively charged wall, producing another form of chain reaction, electrical arcing, and breakdown.

The reasons electric actuators and motors are so attractive on the scale of MEMS, but almost never used at larger scales, are therefore that: 1) the breakdown field strength E_B increases approximately two orders of magnitude for micron-sized gaps, enabling force densities up to four orders of magnitude greater than usual, and 2) enormous values for E and pressure can be achieved with reasonable voltages across micron or sub-micron gaps ($\Rightarrow \sim 3\times 10^8$ [V m^{-1}] and ~10 lb/cm^2).

The breakdown fields for materials are problematic because any local defect can concentrate field strengths locally, exceeding the threshold. Fields of $\sim 10^6$ Vm^{-1} are a nominal upper bound, although somewhat higher values are obtained in integrated circuits.

6.3 Rotary magnetic motors

6.3.1 Commutated rotary magnetic motors

Most *electric motors* and generators are rotary because their motion can then be continuous and high velocity, which improves power density and efficiency while prolonging equipment life. Figure 6.3.1 illustrates an idealized motor with a rotor comprising a single loop of wire carrying current I in the uniform magnetic field $\overline{H}$. The magnetic field can originate from permanent magnets in the stationary *stator*, which is the magnetic structure within which the rotor rotates, or from currents flowing in wires wrapped around the stator. The rotor typically has many turns of wire, often wrapped around a steel core with poles that nearly contact the stator along a cylindrical surface.

The total torque (force times radius) on the motor axle is found by adding the contributions from each of the four sides of the current loop; only the longitudinal elements of length W at radius $\bar{r}$ contribute, however. This total *torque vector* $\overline{T} = \bar{f} \times \bar{r}$ is the integral of the torque contributions from the force density F acting on each incremental length ds of the wire along its entire contour C:

$$\overline{T} = \oint_C \bar{r} \times \overline{F}\, ds \qquad \text{(torque on rotor)} \qquad (6.3.1)$$

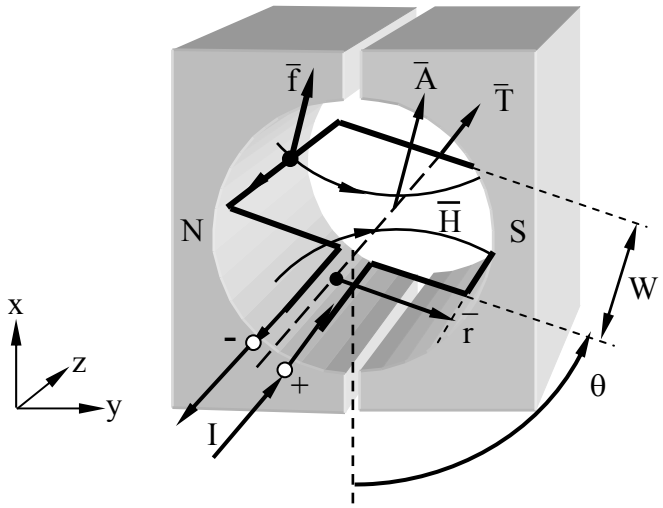

Figure 6.3.1 Rotary single-turn magnetic motor.

The force density $\bar{F}$ [N m^{-1}] on a wire conveying current $\bar{I}$ in a magnetic field $\bar{H}$ follows from the Lorentz force equation (5.1.1) and was given by (5.2.7):

$$\bar{F} = \bar{I} \times \mu_o \bar{H} \left[N\,m^{-1} \right] \qquad \text{(force density on wire)} \qquad (6.3.2)$$

Thus the torque for this motor at the pictured instant is clockwise and equals:

$$\bar{T} = \hat{z} 2rI\mu_o HW \left[N\,m \right] \qquad (6.3.3)$$

In the special case where $\bar{H}$ is uniform over the coil area $A_o = 2rW$, we can define the *magnetic moment* $\bar{M}$ of the coil, where $|\bar{M}| = IA_o$ and where the vector $\bar{M}$ is defined in a right hand sense relative to the current loop $\bar{I}$. Then:

$$\bar{T} = \bar{M} \times \mu_o \bar{H} \qquad (6.3.4)$$

Because the current flows only in the given direction, $\bar{H}$ and the torque reverse as the wire loop passes through vertical ($\theta = n\pi$) and have zero average value over a full rotation. To achieve positive average torque, a *commutator* can be added, which is a mechanical switch on the rotor that connects one or more rotor windings with one or more stationary current sources in the desired sequence and polarity. The commutator reverses the direction of current at times chosen so as to maximize the average positive torque. A typical configuration is suggested in Figure 6.3.2(a) where two spring-loaded carbon brushes pass the current I to the commutator contacts, which are rigidly attached to the rotor so as to reverse the current polarity twice per revolution. This yields the more nearly constant torque history $T(\theta)$ illustrated by the dashed line in Figure 6.3.2(b). In this approximate analysis of a DC motor we assume that the time

constant L/R associated with the rotor inductance L and circuit resistance R is short compared to the torque reversals illustrated in Figure 6.3.2(b).

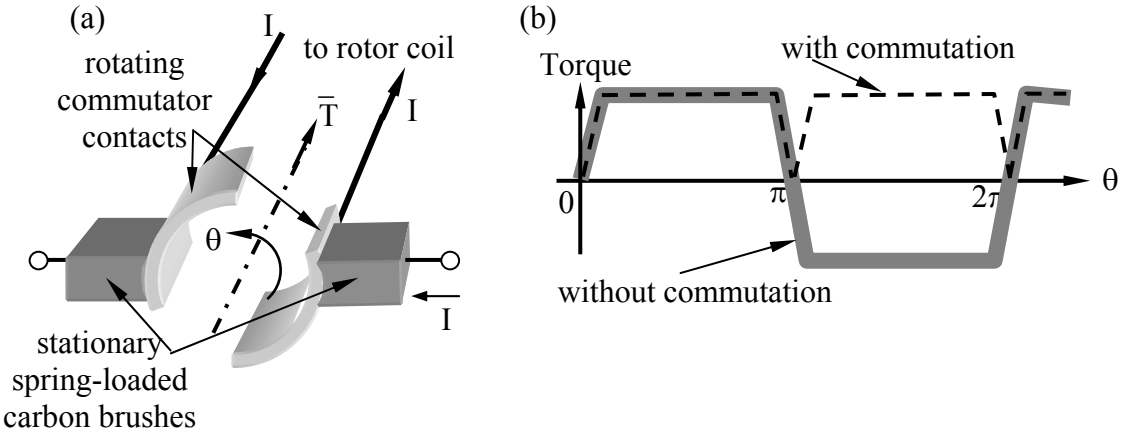

Figure 6.3.2 Commutator motor torque history and contact configuration.

Power is conserved, so if the windings are lossless then the average electrical power delivered to the motor, $P_e = \langle VI \rangle$, equals the average mechanical power delivered to the environment:

$$P_m = f_m v_m = f_m r_m \omega = T\omega \tag{6.3.5}$$

where v_m is the velocity applied to the motor load by force f_m at radius r_m. If the motor is driven by a current source I, then the voltage across the rotor windings in this lossless case is:

$$V = P_e/I = P_m/I = T\omega/I \tag{6.3.6}$$

This same voltage V across the rotor windings can also be deduced from the Lorentz force $\bar{f} = q\left(\bar{E} + \bar{v} \times \mu_o \bar{H}\right)$, (6.1.1), acting on free conduction electrons within the wire windings as they move through $\bar{H}$. For example, if the motor is open circuit ($I \equiv 0$), these electrons spinning about the rotor axis at velocity $\bar{v}$ will move along the wire due to the "$q\bar{v} \times \mu_o \bar{H}$" force on them until they have charged parts of that wire relative to other parts so as to produce a "$q\bar{E}$" force that balances the local magnetic force, producing equilibrium and zero additional current. Free electrons in equilibrium have repositioned themselves so they experience no net Lorentz force. Therefore:

$$\bar{E} = -\bar{v} \times \mu_o \bar{H} \quad \left[\mathrm{V\ m^{-1}}\right] \qquad \text{(electric field inside moving conductor)} \tag{6.3.7}$$

The integral of $\bar{E}$ from one end of the conducting wire to the other yields the open-circuit voltage Φ, which is the Thevenin voltage for this moving wire and often called the *motor back-*

voltage. Φ varies only with rotor velocity and H, independent of any load. For the motor of Figure 6.3.1, Equation (6.3.7) yields the open-circuit voltage for a one-turn coil:

$$\Phi = 2EW = 2v\mu_o HW = 2\omega r\mu_o HW = \omega A_o \mu_o H \quad [V] \qquad \text{(motor back-voltage)} \qquad (6.3.8)$$

where the single-turn coil area is $A_o = 2rW$. If the coil has N turns, then A_o is replaced by NA_o in (6.3.8).

The Thevenin equivalent circuits representing the motor and its external circuit determine the current I, as illustrated in Figure 6.3.3.

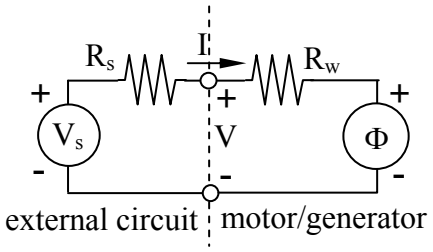

Figure 6.3.3 Equivalent circuit for a driven motor/generator.

R_w is the winding resistance of the motor, where:

$$I = \left(V_S - \Phi\right) \Big/ \left(R_S + R_W\right) \qquad \text{(motor current)} \qquad (6.3.9)$$

When the motor is first starting, $\omega = \Phi = 0$ and the current and the torque are maximum, where $I_{max} = V_s/(R_s + R_w)$. The maximum torque, or "starting torque" from (6.3.3), where $A_o = 2rW$ and there are N turns, is:

$$\overline{T}_{max} = \hat{z}2WrNI_{max}\mu_o H = \hat{z}NA_o I_{max}\mu_o H \quad [Nm] \qquad (6.3.10)$$

Since $\Phi = 0$ when $\overline{v} = 0$, $I\Phi = 0$ and no power is converted then. As the motor accelerates toward its maximum ω, the back-voltage Φ steadily increases until it equals the source voltage V_s so that the net driving voltage, torque T, and current $I \to 0$ at $\omega = \omega_{max}$. Since (6.3.8) says $\Phi = \omega NA_o\mu_o H$, it follows that if $\Phi = V_s$, then:

$$\omega_{max} = \frac{V_S}{NA_o\mu_o H} = \frac{V_S I_{max}}{T_{max}} \qquad (6.3.11)$$

where the relation to T_{max} comes from (6.3.10), and ω_{max} occurs at $T_{min.} = 0$. At ω_{max} no power is being converted, so the maximum motor power output P_{max} occurs at an intermediate speed ω_p, as illustrated in Figure 6.3.4.

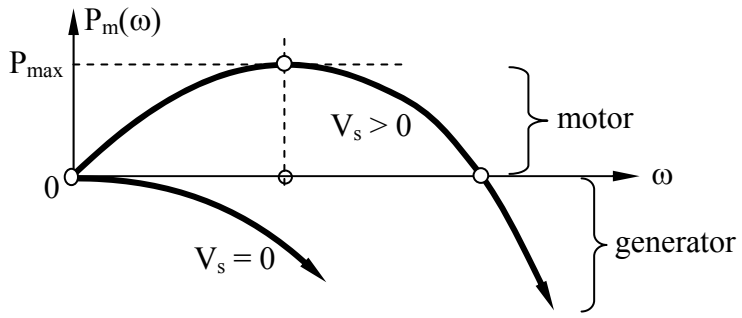

Figure 6.3.4 Mechanical power output $P_m(\omega)$ from a magnetic motor.

An expression for the mechanical output power $P_m(\omega)$ follows from (6.3.9):

$$P_m = T\omega = I\Phi = \left(V_s\Phi - \Phi^2\right)\Big/\left(R_s + R_w\right) \qquad \text{(mechanical power out)} \qquad (6.3.12)$$

where (6.3.8) says $\Phi = \omega N A_o \mu_o H$, so $P_m \propto (V_s\omega - N A_o \mu_o H \omega^2)$.

Equation (6.3.12) says that if $V_s >> \Phi$, which occurs for modest values of ω, then the motor power increases linearly with Φ and ω. Also, if $V_s = 0$, then P_m is negative and the device acts as a *generator* and transfers electrical power to $R_s + R_w$ proportional to Φ^2 and therefore ω^2. Moreover, if we differentiate P_m with respect to Φ and set the result to zero, we find that the mechanical power is greatest when $\Phi = V_s/2$, which implies $\omega_p = \omega_{max}/2$. In either the motor or generator case, the maximum power transfer is usually limited by currents overheating the insulation or by high voltages causing breakdown. Even when no power is transferred, the back-voltage Φ could cause breakdown if the device spins too fast. Semiconductor switches that may fail before the motor insulation are increasingly replacing commutators so the risk of excessive ω is often a design issue. In an optimum motor design, all failure types typically occur near the same loading levels or levels of likelihood.

Typical parameters for a commutated 2-inch motor of this type might be: 1) $B = \mu_o H = 0.4$ Tesla (4000 gauss) provided by permanent magnets in the stator, 2) an $N = 50$-turn coil on the rotor with effective area $A = 10^{-3}N$ [m^2], 3) $V_s = 24$ volts, and 4) $R_s + R_w = 0.1$ ohm. Then it follows from (6.3.11), (6.3.12) for $\Phi = V_s/2$, and (6.3.10), respectively, that:

$$\omega_{max} = V_s/\mu_o HAN = 24\Big/\left(0.4\times10^{-3}\times50\right) = 1200\ \left[\text{rs}^{-1}\right] \Rightarrow 11{,}460\ [\text{rpm}]^{25} \qquad (6.3.13)$$

$$P_{max} = \left(V_s\Phi - \Phi^2\right)\Big/\left(R_s + R_w\right) = V_s^2\Big/\left[4\left(R_s + R_w\right)\right]\left[\text{W}\right] = 24^2/0.4 \cong 1.4\left[\text{kW}\right] \qquad (6.3.14)$$

$$T_{max} = AN\mu_o HI_{max} = A\mu_o HV_s\Big/\left(R_s + R_w\right) = 0.05\times0.4\times24/0.1 = 4.8\ \left[\text{Nm}\right] \qquad (6.3.15)$$

[25] The abbreviation "rpm" means revolutions per minute.

In practice, most motors like that of Figure 6.3.1 wrap the rotor windings around a high permeability core with a thin gap between rotor and stator; this maximizes H near the current I. Also, if the unit is used as an AC generator, then there may be no need for the polarity-switching commutator if the desired output frequency is simply the frequency of rotor rotation.

Example 6.3A

Design a commutated DC magnetic motor that delivers maximum mechanical power of 1 kW at 600 rpm. Assume B = 0.2 Tesla and that the source voltage V_s = 50 volts.

Solution: Maximum mechanical power is delivered at $\omega_p = \omega_{max}/2$ (see Figure 6.3.4). Solving (6.3.13) yields $NA_o = V_s/(\omega_{max}\mu_o H) = 50/(2\times600\times60\times2\pi\times0.2) = 5.53\times10^{-4}$, where ω_{max} corresponds to 1200 rpm. If N = 6, then the winding area $2rW = A_o \cong 1$ cm^2. To find I_{max} we use (6.3.14) to find the maximum allowed value of $R_s + R_w = (V_s\Phi - \Phi^2)/P_m$. But when the delivered mechanical power P_{mech} is maximum, $\Phi = V_s/2$, so $R_s + R_w = (50\times25 - 25^2)/10^3 = 0.63\Omega$, which could limit N if the wire is too thin. $I_{max} = V_s/(R_s + R_w) = 50/0.63 = 80$ [A]. The starting torque $T_{max} = I_{max}(NA_o)\mu_o H = 80(5.53\times10^{-4})0.2 = 0.22$ [N m]. This kilowatt motor occupies a fraction of a cubic inch and may therefore overheat because the rotor is small and its thermal connection with the external world is poor except through the axle. It is probably best used in short bursts between cooling-off periods. The I^2R_w thermal power dissipated in the rotor depends on the wire design.

6.3.2 Reluctance motors

Reluctance motors combine the advantages of rotary motion with the absence of rotor currents and the associated rotary contacts. Figure 6.3.5 suggests a simple idealized configuration with only a single drive coil.

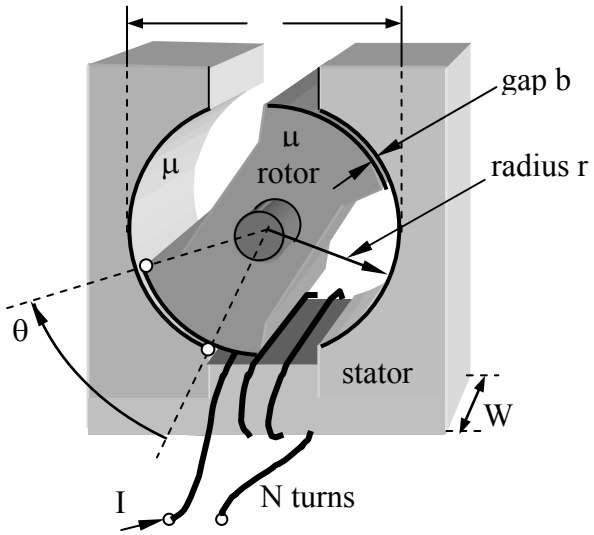

Figure 6.3.5 Two-pole single-winding reluctance motor.

When the coil is energized the rotor is pulled by the magnetic fields into alignment with the magnetic fields linking the two poles of the stator, where $\mu >> \mu_o$ in both the rotor and stator. Reluctance motors must sense the angular position of the rotor, however, so the stator winding(s) can be excited at the right times so as to pull the passive high-μ rotor toward its next rotary position, and then not retard it as it moves on toward the following attractive position. For example, the current I in the figure will pull the rotor so as to increase θ, which is the overlap angle between the rotor and the stator poles. Once the overlap is complete the current I would be set to zero as the rotor coasts until the poles again have $\theta \cong 0$ and are in position to be pulled forward again by I. Such motors are efficient if hysteresis losses in the stator and rotor are modest and the stator windings are nearly lossless.

The torque on such a reluctance motor can be readily calculated using (6.2.12):

$$T = -dw_T/d\theta \ \ [\mathrm{N\,m}] \tag{6.3.16}$$

The total magnetic energy w_T includes w_μ within the rotor and stator, w_g in the air gaps between them, and any energy in the power supply driving the motor. Fortunately we can simplify the problem by noting that w_g generally dominates, and that by short-circuiting the stator the same torque exists without any power source if I remains unchanged.

The circumstances for which the gap energy dominates the total energy w_T are easily found from the static integral form of Ampere's law (1.4.1):

$$NI = \oint_C \left(\overline{H}_{gap} + \overline{H}_{stator} + \overline{H}_{rotor}\right) \bullet d\bar{s} \cong 2bH_{gap} \tag{6.3.17}$$

To derive an approximate result we may assume the coil has N turns, the width of each gap is b, and the contour C threads the coil and the rest of the motor over a distance ~2D, and through an approximately constant cross-section A; D is the rotor diameter. Since the boundary conditions in each gap require $\overline{B}_\perp$ be continuous, $\mu H_\mu \cong \mu_o H_g$, where $H_\mu \cong H_{stator} \cong H_{rotor}$ and $H_g \equiv H_{gap}$. The relative energies stored in the two gaps and the rotor/stator are:

$$w_g \cong 2bA\left(\mu_o H_g^2/2\right) \tag{6.3.18}$$

$$w_{r/s} \cong 2DA\left(\mu H_\mu^2/2\right) \tag{6.3.19}$$

Their ratio is:

$$w_g/w_{r/s} = 2b\left(\mu_o/\mu\right)\left(H_g/H_\mu\right)^2/2D = b\left(\mu/\mu_o\right)/D \tag{6.3.20}$$

Thus $w_g >> w_\mu$ if $b/D >> \mu_o/\mu$. Since gaps are commonly $b \cong 100$ microns, and iron or steel is often used in reluctance motors, $\mu \cong 3000$, so gap energy w_g dominates if the motor diameter D << 0.3 meters. If this approximation doesn't apply then the analysis becomes somewhat more

complex because both energies must be considered; reluctance motors can be much larger than 0.3 meters and still function.

Under the approximations $w_T \cong w_g$ and A = gap area = $r\theta W$, we may compute the torque T using (6.3.16) and (6.3.18):[26]

$$T = -dw_g/d\theta = -b\mu_o d\left(A\left|H_g\right|^2\right)\Big/d\theta \tag{6.3.21}$$

The θ dependence of H_g can be found from Faraday's law by integrating $\bar{E}$ around the short-circuited coil:

$$\oint_{c\ coil} \bar{E} \bullet d\bar{s} = -N\iint_A \left(d\bar{B}/dt\right) \bullet d\bar{a} = -d\Lambda/dt = 0 \tag{6.3.22}$$

The flux linkage Λ is independent of θ and constant around the motor [contour C of (6.3.17)], so Λ, w_g and T are easily evaluated at the gap where the area is A = $r\theta W$:

$$\Lambda = N\int_A \bar{B} \bullet d\bar{a} = NB_g A = N\mu_o H_g r\theta W \tag{6.3.23}$$

$$w_g = 2\left(\mu_o {H_g}^2/2\right)bA = b\Lambda^2\Big/\left(N^2\mu_o r\theta W\right) \tag{6.3.24}$$

$$T = -dw_g/d\theta = b\Lambda^2\Big/\left(N^2\mu_o rW\theta^2\right) = r2\left(\mu_o {H_g}^2/2\right)\text{Wb}\ \left[\text{N m}\right] \tag{6.3.25}$$

The resulting torque T in (6.3.25) can be interpreted as being the product of radius r and twice the force exerted at the leading edge of each gap (twice, because there are two gaps), where this force is the *magnetic pressure* $\mu_o {H_g}^2/2$ [N m^{-2}] times the gap area Wb projected on the direction of motion. Because the magnetic field lines are perpendicular to the direction of force, the magnetic pressure pushes rather than pulls, as it would if the magnetic field were parallel to the direction of force. Unfortunately, increasing the gap b does not increase the force, because it weakens H_g proportionately, and therefore weakens $T \propto H^2$. In general, b is designed to be minimum and is typically limited to roughly 25-100 microns by thermal variations and bearing and manufacturing tolerances. The magnetic field in the gap is limited by the saturation field of the magnetic material, as discussed in Section 2.5.4.

The drive circuits initiate the current I in the reluctance motor of Figure 6.3.5 when the gap area $r\theta W$ is minimum, and terminate it when that area becomes maximum. The rotor then coasts with I = 0 and zero torque until the area is again minimum, when the cycle repeats. Configurations that deliver continuous torque are more commonly used instead because of their smoother performance.

[26] The approximate dependence (6.3.19) of $w_{r/s}$ upon A = $r\theta W$ breaks down when $\theta \to 0$, since w_g doesn't dominate then and (6.3.19) becomes approximate.

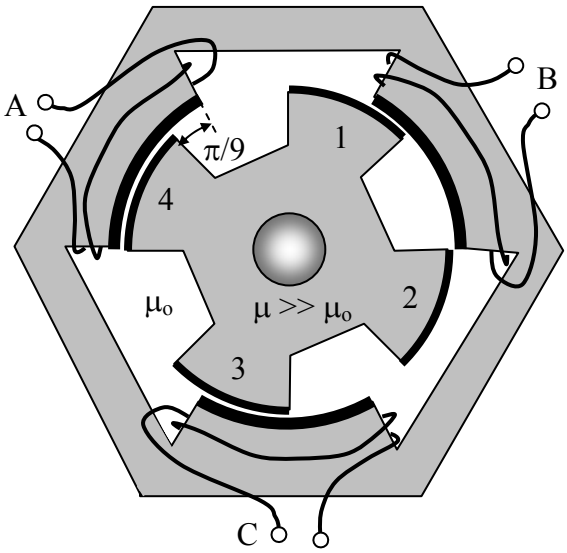

Figure 6.3.6 Reluctance motor with 3 stator and 4 rotor poles.

Figure 6.3.6 illustrates a reluctance motor that provides continuous torque using three stator poles (A, B, C) and four rotor poles (1, 2, 3, 4). When windings A and B are excited, rotor pole 1 is pulled clockwise into stator pole B. The gap area for stator pole A is temporarily constant and contributes no additional torque. After the rotor moves $\pi/9$ radians, the currents are switched to poles B and C so as to pull rotor pole 2 into stator pole C, while rotor pole 1 contributes no torque. Next C and A are excited, and this excitation cycle (A/B, B/C, C/A) is repeated six times per revolution. Counter-clockwise torque is obtained by reversing the excitation sequence. Many pole combinations are possible, and those with more poles yield higher torques because torque is proportional to the number of active poles. In this case only one pole is providing torque at once, so the constant torque $T = bW(\mu_o H_g^2/2)$ [N m].

A calculation very similar to that above also applies to *relays* such as that illustrated in Figure 6.3.7, where a coil magnetizes a flexible or hinged bar, drawing it downward to open and/or close one or more electrical contacts.

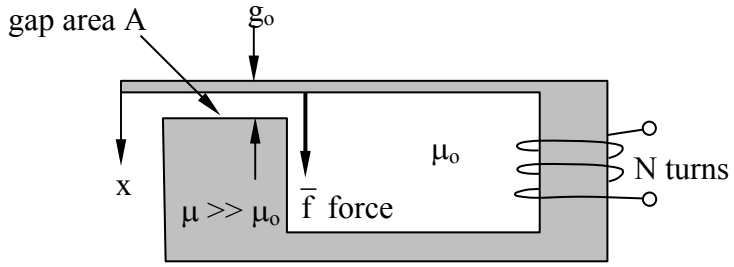

Figure 6.3.7 Magnetic relay.

We can find the force f, flux linkage Λ, and gap energy w_g using a short-circuited N-turn coil to render Λ constant, as before:

$$f = -dw_g/dx \qquad \text{(force closing the gap)} \qquad (6.3.26)$$

$$\Lambda = N\mu_o H_g A \qquad \text{(flux linkage)} \qquad (6.3.27)$$

$$w_g = (\mu_o H_g^2/2)A(g_o - x) = (g_o - x)\Lambda^2/(2N^2\mu_o A) \ \text{[J]} \qquad \text{(gap energy)} \qquad (6.3.28)$$

$$f = -dw_g/dx = \Lambda^2/(2N^2\mu_o A) = (\mu_o H_g^2/2)A \ \text{[N]} \qquad \text{(force)} \qquad (6.3.29)$$

This force can also be interpreted as the gap area A times a *magnetic pressure* P_m, where:

$$P_m = \mu_o H_g^2/2 \quad [N/m^2] \qquad \text{(magnetic pressure)} \qquad (6.3.30)$$

The magnetic pressure is attractive parallel to the field lines, tending to close the gap. The units N/m^2 are identical to J/m^3. Note that the minus sign is used in (6.3.29) because f is the magnetic force closing the gap, which equals the mechanical force required to hold it apart; motion in the x direction reduces w_g.

Magnetic micro-rotary motors are difficult to build without using magnetic materials or induction[27] because it is difficult to provide reliable sliding electrical contacts to convey currents to the rotor. One form of rotary magnetic motor is similar to that of Figures 6.2.3 and 6.2.4, except that the motor pulls into the segmented gaps a rotating high-permeability material instead of a dielectric, where the gaps would have high magnetic fields induced by stator currents like those in Figure 6.3.6. As in the case of the rotary dielectric MEMS motors discussed in Section 6.2, the timing of the currents must be synchronized with the angular position of the rotor. The force on a magnetic slab moving into a region of strong magnetic field can be shown to approximate $A\mu H_\mu^2/2$ [N], where A is the area of the moving face parallel to H_μ, which is the field within the moving slab, and $\mu >> \mu_o$. The rotor can also be made permanently magnetic so it is attracted or repelled by the synchronously switched stator fields; permanent magnet motors are discussed later in Section 6.5.2.

Example 6.3B

A relay like that of Figure 6.3.7 is driven by a current source I [A] and has a gap of width g. What is the force f(g) acting to close the gap? Assume the cross-sectional area A of the gap and metal is constant around the device, and note the force is depends on whether the gap is open or closed.

Solution: This force is the pressure $\mu_o H_g^2/2$ times the area A (6.3.29), assuming $\mu >> \mu_o$. Since $\nabla \times \overline{H} = \overline{J}$, therefore $NI = \oint H(s)\, ds = H_g g + H_\mu S$, where S is the path length around the loop having permeability μ. When $H_g g >> H_\mu S$, then $H_g \cong NI/g$ and $f \cong$

[27] Induction motors, not discussed in this text, are driven by the magnetic forces produced by a combination of rotor and stator currents, where the rotor currents are induced by the time-varying magnetic fields they experience, much like a transformer. This avoids the need for direct electrical contact with the rotor.

$\mu_o(NI/g)^2A/2$ for the open relay. When the relay is closed and g ≅0, then $H_g \cong \mu H_u/\mu_o$, where $H_\mu \cong NI/S$; then $f \cong (\mu NI/S)^2A/2\mu_o$. The ratio of forces when the relay is closed to that when it is open is $(\mu g/\mu_o S)^2$, provided $H_g g >> H_\mu S$ and this ratio >> 1.

6.4 Linear magnetic motors and actuators

6.4.1 Solenoid actuators

Compact actuators that flip latches or switches, increment a positioner, or impact a target are often implemented using solenoids. *Solenoid actuators* are usually cylindrical coils with a slideably disposed high-permeability cylindrical core that is partially inserted at rest, and is drawn into the solenoid when current flows, as illustrated in Figure 6.4.1. A spring (not illustrated) often holds the core near its partially inserted rest position.

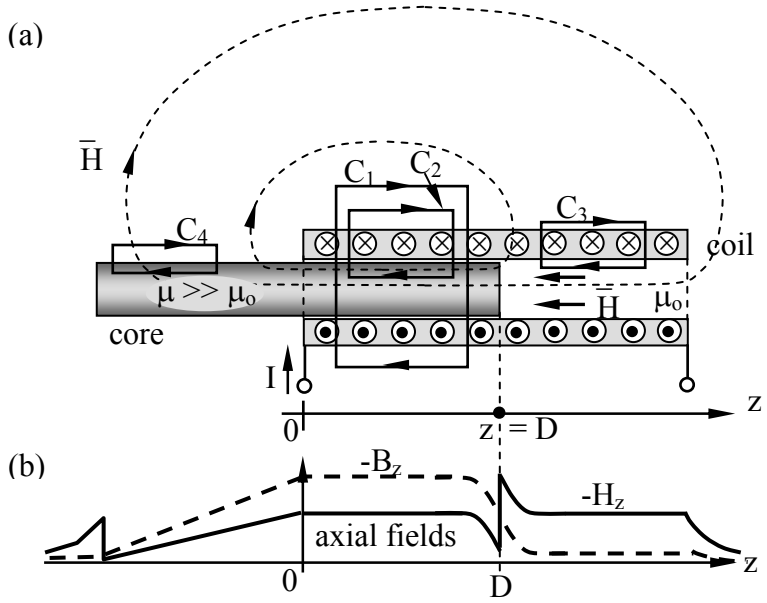

Figure 6.4.1 Solenoid actuator and fields (B and H are plotted on different scales).

If we assume the diameter of the solenoid is small compared to its length, then the fringing fields at the ends of the coil and core can be neglected relative to the field energy stored elsewhere along the solenoid. If we integrate $\overline{H}$ along contour C_1 (see figure) we obtain zero from Ampere's law because no net current flows through C_1 and $\partial\overline{D}/\partial t \cong 0$:

$$\oint_C \overline{H} \bullet d\bar{s} = \iint_A \left(\bar{J} + \partial\overline{D}/\partial t\right) \bullet \hat{n}\ da = 0 \tag{6.4.1}$$

This implies $\overline{H} \cong 0$ outside the solenoid unless H_z is approximately uniform outside, a possibility that is energetically disfavored relative to H being purely internal to the coil. Direct evaluation

of $\overline{H}$ using the Biot-Savart law (1.4.6) also yields $\overline{H} \cong 0$ outside. If we integrate $\overline{H}$ along contour C_2, which passes along the axis of the solenoid for unit distance, we obtain:

$$\oint_{C2} \overline{H} \bullet d\bar{s} = N_o I = -H_z \tag{6.4.2}$$

where N_o is defined as the number of turns of wire per meter of solenoid length. We obtain the same answer (6.4.2) regardless of the permeability along the contour C_2, provided we are not near the ends of the solenoid or its moveable core. For example, (6.4.2) also applies to contour C_3, while the integral of $\overline{H}$ around C_4 is zero because the encircled current there is zero.

Since (6.4.2) requires that H_z along the solenoid axis be approximately constant, B_z must be a factor of μ/μ_o greater in the permeable core than it is in the air-filled portions of the solenoid. Because boundary conditions require $\overline{B}_\perp$ to be continuous at the core-air boundary, $\overline{H}_\perp$ must be discontinuous there so that $\mu H_\mu = \mu_o H_o$, where H_μ and H_o are the axial values of H in the core and air, respectively. This appears to conflict with (6.4.2), which suggests $\overline{H}$ inside the solenoid is independent of μ, but this applies only if we neglect fringing fields at the ends of the solenoid or near boundaries where μ changes. Thus the axial H varies approximately as suggested in Figure 6.4.1(b): it has a discontinuity at the boundary that relaxes toward constant H = $N_o I$ away from the boundary over a distance comparable to the solenoid diameter. Two representative field lines in Figure 6.4.1(a) suggest how $\overline{B}$ diverges strongly at the end of the magnetic core within the solenoid while other field lines remain roughly constant until they diverge at the right end of the solenoid. The transition region between the two values of B_z at the end of the solenoid occurs over a distance roughly equal to the solenoid diameter, as suggested in Figure 6.4.1(b). The magnetic field lines $\overline{B}$ and $\overline{H}$ "repel" each other along the protruding end of the high permeability core on the left side of the figure, resulting in a nearly linear decline in magnetic field within the core there; at the left end of the core there is again a discontinuity in $|H_z|$ because $\overline{B}_\perp$ must be continuous.

Having approximated the field distribution we can now calculate energies and forces using the expression for magnetic energy density, $W_m = \mu H^2/2$ [J m^{-3}]. Except in the negligible fringing field regions at the ends of the solenoid and at the ends of its core, $|H| \cong N_o I$ (6.4.2) and $\mu H^2 >> \mu_o H^2$, so to simplify the solution we neglect the energy stored in air as we compute the magnetic force f_z pulling on the core in the +z direction:

$$f_z = -dw_T/dz \ \ [N] \tag{6.4.3}$$

The energy in the core is confined largely to the length z within the solenoid, which has a cross-sectional area A [m^2]. The total magnetic energy w_m thus approximates:

$$w_m \cong Az\mu H^2/2 \ \ [J] \tag{6.4.4}$$

If we assume $w_T = w_m$ and differentiate (6.4.4) assuming H is independent of z, we find the magnetic force expels the core from the solenoid, the reverse of the truth. To obtain the correct answer we must differentiate the total energy w_T in the system, which includes any energy in the

power source supplying the current I. To avoid considering a power supply we may alternatively assume the coil is short-circuited and carrying the same I as before. Since the instantaneous force on the core depends on the instantaneous I and is the same whether it is short-circuited or connected to a power source, we may set:

$$v = 0 = d\Lambda/dt \tag{6.4.5}$$

where:

$$\Lambda \cong N\psi_m = N\iint_A \mu\overline{H}_\mu \bullet d\overline{a} = N_o z\, \mu H_\mu A \tag{6.4.6}$$

H_μ is the value of H inside the core (μ) and $N_o z$ is the number of turns of wire circling the core, where N_o is the number of turns per meter of coil length. But $H_\mu = J_s$ [A m^{-1}] = $N_o I$, so:

$$\Lambda = N_o^2 Iz\mu A \tag{6.4.7}$$

$$I = \Lambda \Big/ \left(N_o^2 z\mu A \right) \tag{6.4.8}$$

We now can compute w_T using only w_m because we have replaced the power source with a short circuit that stores no energy:

$$w_T \cong \mu H_\mu^2 Az/2 = \mu\left(N_o I\right)^2 Az/2 = \mu\left(\Lambda/\mu N_o Az\right)^2 Az/2 = \Lambda^2 \Big/ \left(\mu N_o^2 Az2\right) \tag{6.4.9}$$

So (6.4.9) and (6.4.6) yield the force pulling the core into the solenoid:

$$f_z = -\frac{dw_T}{dz} = -\frac{d}{dz}\left[\frac{\Lambda^2}{\mu N_o^2 2Az}\right] = \frac{(\Lambda/N_o z)^2}{2A\mu} = \frac{\mu H_\mu^2 A}{2} \quad [N] \tag{6.4.10}$$

where $H_\mu = H$. This force is exactly the area A of the end of the core times the same magnetic pressure $\mu H^2/2$ [Nm^{-2}] we saw in (6.3.25), but this time the magnetic field is pulling on the core in the direction of the magnetic field lines, whereas before the magnetic field was pushing perpendicular to the field lines. This pressure equals the magnetic energy density W_m, as before. A slight correction for the non-zero influence of μ_o and associated small pressure from the air side could be made here, but more exact answers to this problem generally also require consideration of the fringing fields and use of computer tools.

It is interesting to note how electric and magnetic pressure [N/m^2] approximates the energy density [J m^{-3}] stored in the fields, where we have neglected the pressures applied from the low-field side of the boundary when $\varepsilon >> \varepsilon_o$ or $\mu >> \mu_o$. We have now seen examples where $\overline{E}$ and $\overline{H}$ both push or pull on boundaries from the high-field (usually air) side of a boundary, where both $\overline{E}$ and $\overline{H}$ pull in the direction of their field lines, and push perpendicular to them.

6.4.2 MEMS magnetic actuators

One form of magnetic MEMS switch is illustrated in Figure 6.4.2. A control current I_2 deflects a beam carrying current I_1. When the beam is pulled down toward the substrate, the switch (not shown) will close, and when the beam is repelled upward the switch will open. The Lorentz force law (1.2.1) states that the magnetic force $\bar{f}$ on a charge q is $q\bar{v}\times\mu_o\overline{H}$, and therefore the force density per unit length $\bar{F}$ [N m^{-1}] on a current $\bar{I}_1 = Nq\bar{v}$ induced by the magnetic field $\overline{H}_{12}$ at position 1 produced by I_2 is:

$$\bar{F} = Nq\bar{v}\times\mu_o\overline{H}_{12} = \bar{I}_1\times\mu_o\overline{H}_{12}\ \left[\mathrm{Nm^{-1}}\right] \tag{6.4.11}$$

N is the number of moving charges per meter of conductor length, and we assume that all forces on these charges are conveyed directly to the body of the conductor.

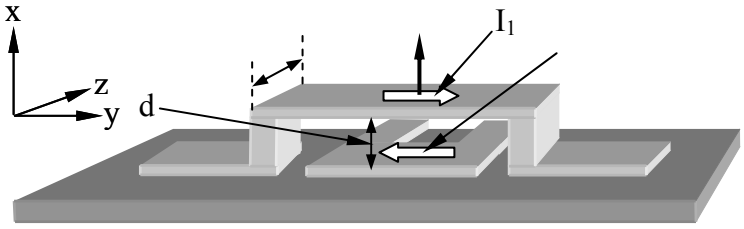

Figure 6.4.2 Magnetic MEMS switch.

If the plate separation d << W, then fringing fields can be neglected and the I_2-induced magnetic field affecting current I_1 is $\overline{H}_{12}$, which can be found from Ampere's law (1.4.1) computed for a contour C circling I_2 in a right-hand sense:

$$\oint_C \overline{H}\bullet d\bar{s} \cong H_{12}\,2W = \iint_A \bar{J}\bullet\hat{n}\,da = I_2 \tag{6.4.12}$$

Thus $\overline{H}_{12} \cong \hat{z}I_2/2W$. The upward pressure on the upper beam found from (6.4.11) and (6.4.12) is then:

$$\bar{P} = \bar{F}/W \cong \hat{x}\mu_o I_1 I_2/2W^2\ \left[\mathrm{N\,m^{-2}}\right] \tag{6.4.13}$$

If I_1 = -I_2 then the magnetic field between the two closely spaced currents is $H_o' = I_1/W$ and (6.4.13) becomes $\bar{p} = \hat{x}\mu_o H_o'^2/2$ [N m^{-2}]; this expression for magnetic pressure is derived differently in (6.4.15).

This pressure on the top is downward if both currents flow in the same direction, upward if they are opposite, and zero if either is zero. This device therefore can perform a variety of logic functions. For example, if a switch is arranged so its contacts are closed in state "1" when the

beam is forced upward by both I_1 and I_2 being positive (these currents were defined in the figure as flowing in opposite directions), and not otherwise, this is an "and" gate.

An alternate way to derive magnetic pressure (6.4.13) is to note that if the two currents I_1 and I_2 are anti-parallel, equal, and close together (d << W), then $\bar{H} = 0$ outside the two conductors and H_o' is doubled in the gap between them so $WH_o' = I_1$. That is, if the integration contour C circles either current alone then (6.4.12) becomes:

$$\oint_C \bar{H} \bullet d\bar{s} \cong H_o' W = \iint_A \bar{J} \bullet \hat{n}\, da = I_1 = I_2 \tag{6.4.14}$$

But not all electrons comprising these currents see the same magnetic field because the currents closer to the two innermost conductor surfaces screen the outer currents, causing the magnetic field to approach zero inside the conductors, as suggested in Figure 6.4.3.

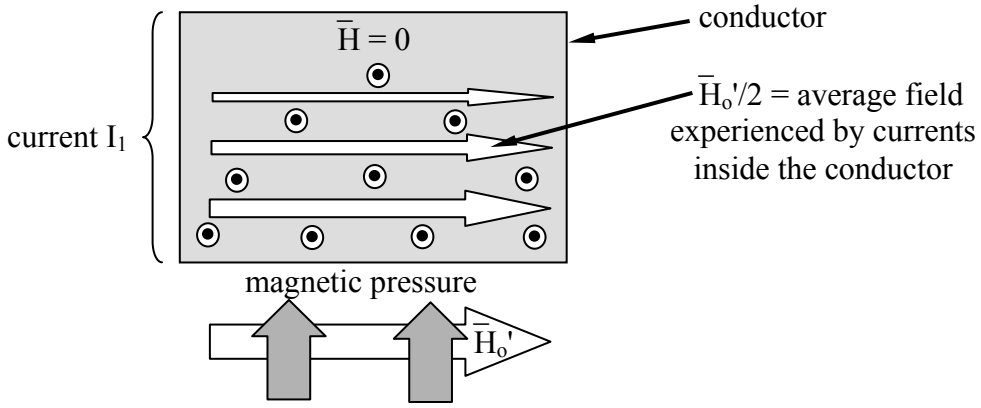

Figure 6.4.3 Surface current and force distribution in a conductor.

Therefore the average moving electron sees a magnetic field $H_o'/2$, half that at the surface[28]. Thus the total *magnetic pressure* upward on the upper beam given by (6.4.13) and (6.4.14) is:

$$\begin{aligned} \bar{P} &= \bar{F}/W = \bar{I}_1 \times \mu_o \bar{H}_o'/2W = \hat{x}\left(H_o' W\right)\left(\mu_o H_o'/2W\right) \\ &= \hat{x}\mu_o H_o'^2/2 \ \left[\mathrm{N\,m^{-2}}\right] \end{aligned} \quad \text{(magnetic pressure)} \tag{6.4.15}$$

where H_o' is the total magnetic field magnitude between the two conductors, and there is no magnetic field on the top of the upper beam to press in the opposite direction. This magnetic pressure [N m^{-2}] equals the magnetic energy density [J m^{-3}] stored in the magnetic field adjacent to the conductor (2.7.8).

[28] A simple integral of the form used in (5.2.4) yields this same result for pressure.

6.5 Permanent magnet devices

6.5.1 Introduction

A *permanent magnet* (Section 2.5.4) has a *residual flux density* $\overline{B}_r$ when $\overline{H} = 0$ inside it, and this is the rest state of an isolated permanent magnet. In this case the magnetic energy density inside is $W_m = \overline{B} \bullet \overline{H}/2 = 0$, and that outside, $W_m = \mu_o |\overline{H}|^2 \neq 0$. Boundary conditions (2.6.5) say $\overline{B}_{r\perp} = \mu_o \overline{H}_{o\perp}$, where $\overline{H}_{o\perp}$ is the boundary value in air. Since $\overline{H}_{//}$ is continuous across an insulating boundary and $\overline{H}_r = 0$ inside a resting permanent magnet, $\overline{H}_{o//} = 0$ too. If an external $\overline{H}$ is applied to a permanent magnet, then $\overline{B}$ within that magnet is altered as suggested by the hysteresis diagram in Figure 2.5.3(b).

The force f [N] attracting a permanent magnet to a high-permeability material can be found using:

$$f = dw_m/dx \tag{6.5.1}$$

where x is the separation between the two, as illustrated in Figure 6.5.1, and w_m is the total energy in the magnetic fields [J]. The changing magnetic energy in the high-permeability material is negligible compared to that in air because: 1) boundary conditions require continuity in $\overline{B}_\perp$ across the boundary so that $\overline{B}_\perp = \mu \overline{H}_\perp = \mu_o \overline{H}_{o\perp}$, and therefore $H_\perp/H_{o\perp} = \mu_o/\mu << 1$, and 2) W_m [Jm^{-3}] $= \mu |\overline{H}|^2/2$ where $\mu >> \mu_o$; thus the energy density in air is greater by $\sim\mu/\mu_o >> 1$.

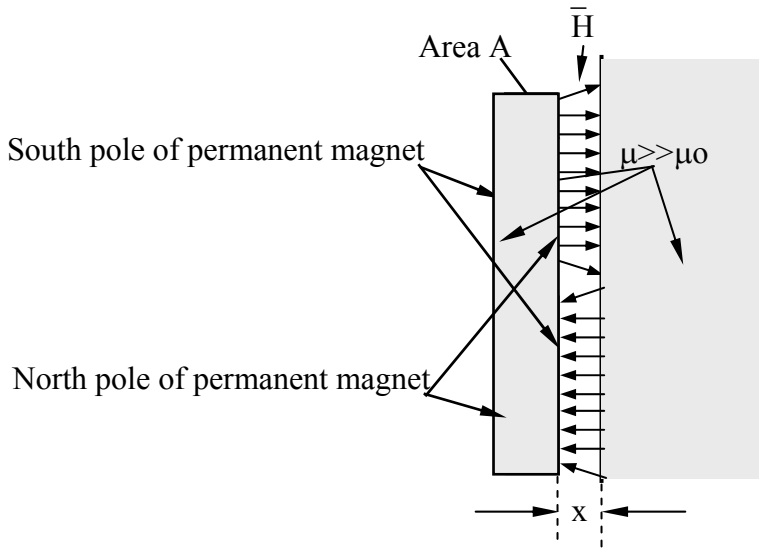

Figure 6.5.1 Permanent magnet adhering to a permeable surface.

The variable magnetic energy is dominated by the energy w_m in the gap, which is the energy density, $W_m = \mu_o H_{gap}^2/2$, times the volume of the gap Ax, where A is the area of the magnet face and x is the gap width. Thus:

$$w_m \cong \mu_o H_{gap}^2 Ax/2 \text{ [J]} \tag{6.5.2}$$

Differentiating w_m with respect to x yields the attractive force $f \cong \mu_o H_{gap}^2 A/2$ [N], and the force density:

$$F \cong \mu_o H_{gap}^2/2 = W_{gap} = B_{gap}^2/2\mu_o \left[\text{J m}^{-3}\right] \tag{6.5.3}$$

This can be expressed in terms of B: $F = B_{gap}^2/2\mu_o$ [Nm^{-2}]. Note that the rest energy density inside the permanent magnet is zero, so it exerts no pressure. Most permanent magnets have magnetic flux densities B less than one Tesla (10^4 gauss), so a magnet this powerful with an area A = 10 cm^2 (~the size of a silver dollar) would therefore apply an attractive force AF = $0.001\times1^2/2\times4\pi10^{-7} \cong 400$N (~100 pound force). A more typical permanent magnet the same size might attract a steel surface with only a 10–20 pound force.

If two equal coin-shaped permanent magnets are stacked so they stick together, then they experience primarily the attractive magnetic pressure $B_{gap}^2/2\mu_o$ [Nm^{-2}] associated with the gap between them, and are bonded with approximately the same force density as if one of them were merely a high-permeability sheet. In this case $B_{gap} \cong B_r$, as shown in Figure 2.5.3(b).

This simple gap-based magnetic pressure model does not explain the repulsive force between two such coin magnets when one is flipped, however, for then $\overline{H}_g \cong 0$ and $w_{gap} \cong 0$ for all small values of x, and dw_g/dx is also ~0. In this case the energy of interest w_T lies largely inside the magnets. This special case illustrates the risks of casually substituting simple models for the underlying physical reality captured in Maxwell's equations, the Lorentz force law, and material characteristics.

Permanent magnets fail above their *Curie temperature* when the magnetic domains become scrambled. Cooling overheated permanent magnets in a strong external magnetic field usually restores them. Some types of permanent magnets can also fail at very low temperatures, and should not be used where that is a risk.

6.5.2 Permanent magnet motors

Compact high-power-density motors often incorporate permanent magnets so current is not wasted on maintenance of $\overline{H}$. For example, the stator for the rotary single-turn coil motor of Figure 6.3.1 could easily contain permanent magnets, avoiding the need for current excitation. Moreover, modern permanent magnets can provide quite intense fields, above 0.5 Tesla. In this case we should also consider the effect of the rotor currents on the stator permanent magnets, whereas in the earlier example we considered the stator fields and rotor currents as given. The

incremental permeability of a permanent magnet varies with the applied H. If H is oriented to attract the stator pole and $\mu_o H > B_r$, then B in the permanent magnet will increase above B_r (see Figure 2.5.3), where the incremental permeability approaches μ_o. To the extent the incremental $\mu > \mu_o$, some reluctance-motor torque will supplement the dominant torque studied earlier.

The permanent magnets can alternatively be placed on the rotor, avoiding the need for rotor currents or a commutator, provided the stator currents are synchronously switched instead. Clever electronics can detect the voltage fluctuations in the stator induced by the rotor and thus deduce its position, potentially avoiding the need for a separate expensive angle encoder for stator current synchronization.

Because different parts of permanent magnets see different B/H histories, and these depend in part on B/H histories elsewhere in the device, modern design of such motors or generators relies extensively on complex software tools for modeling support.

Example 6.5A

Two identical coin-shaped permanent magnets of 12-cm diameter produce 0.05 Tesla field perpendicular to their flat faces; one side is the north pole of the magnet and the other is south. What is the maximum force f attracting the magnets when placed face to face?

Solution: Using (6.5.3) yields $f = AB_{gap}^2/2\mu_o = \pi(0.06)^2(0.05)^2/(2\times1.26\times10^{-6}) = 11.2$ [N].

6.6 Electric and magnetic sensors

6.6.1 Electrostatic MEMS sensors

Sensors are devices that respond to their environment. Some sensors alter their properties as a function of the chemical, thermal, radiation, or other properties of the environment, where a separate active circuit probes these properties. The conductivity, permeability, and permittivity of materials are typically sensitive to multiple environmental parameters. Other sensors directly generate voltages in response to the environment that can be amplified and measured. One common *MEMS sensor* measures small displacements of cantilevered arms due to temperature, pressure, acceleration, chemistry, or other changes. For example, temperature changes can curl a thin cantilever due to differences in thermal expansion coefficient across its thickness, and chemical reactions on the surface of a cantilever can change its mass and mechanical resonance frequency. Microphones can detect vibrations in such cantilevers, or accelerations along specific axes.

Figure 6.6.1 portrays a standard capacitive MEMS sensor that illustrates the basic principles, where the capacitor plates of area A are separated by the distance d, and the voltage V is determined in part by the voltage divider formed by the source resistance R_s and the amplifier input resistance R. V_s is the source voltage.

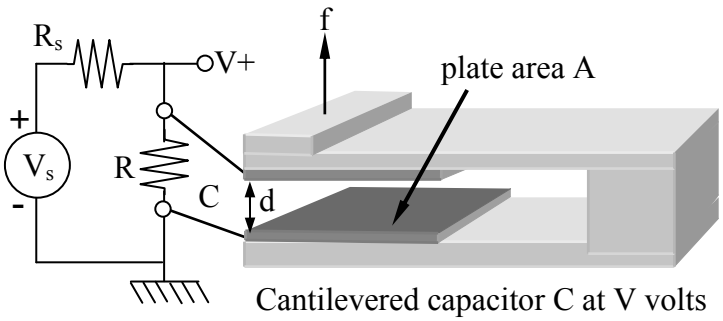

Figure 6.6.1 Capacitive MEMS sensor.

The instantaneous circuit response to an increase δ in the plate separation d is an increase in capacitor voltage V above its normal equilibrium value V_e determined by the voltage divider, where $V_e = V_s R/(R+R_s)$. The capacitor then discharges exponentially toward V_e with a time constant $\tau = (R//R_s)C$.[29] See Section 3.5.1 for further discussions of RC circuit behavior. If $R_s >> R$ then $\tau \cong RC$. If $R_s >> R$ and R represents the input resistance of a high-performance sensor amplifier, then that sensor can detect as little as $\Delta w_B \cong 10^{-20}$ joules per "*bit of information*"[30]. This can be compared to the incremental increase Δw_c in capacitor energy due to the displacement $\delta << d$ as C decreases to C':

$$\Delta w_c = (C - C')V^2/2 = V^2 \varepsilon_o A\left(d^{-1} - [d+\delta]^{-1}\right)/2 \cong V^2 \varepsilon_o A\delta/2d^2 \ \ [J] \qquad (6.6.1)$$

A simple example illustrates the extreme potential sensitivity of such a sensor. Assume the plate separation d is one micron, the plates are 1-mm square ($A = 10^{-6}$), and V = 300. Then the minimum detectable δ given by (6.6.1) for $\Delta w_c = \Delta w_B = 10^{-20}$ Joules is:

$$\begin{aligned} \delta_{min} &= \Delta w_B \times 2d^2/V^2\varepsilon_o A \cong 10^{-20} 2\left(10^{-6}\right)^2 \Big/ \left(300^2 \times 8.8\times 10^{-12} \times 10^{-6}\right) \\ &\cong 2\times 10^{-20} \ \ [m] \end{aligned} \qquad (6.6.2)$$

At this potential level of sensitivity we are limited instead by thermal and mechanical noise due to the Brownian motion of air molecules and conduction electrons. A more practical set of parameters might involve a less sensitive detector ($\Delta_B \cong 10^{-14}$) and lower voltages (V ≅ 5); then $\delta_{min} \cong 10^{-10}$ meters ≅ 1 angstrom (very roughly an atomic diameter). The dynamic range of such a sensor would be enormously greater, of course. This one-angstrom sensitivity is comparable to that of the human eardrum at ~1kHz.

---

[29] The resistance R of two resistors in parallel is $R = (R_a \,||\, R_b) = R_a R_b/(R_a + R_b)$.

[30] Most good communications systems can operate with acceptable probabilities of error if $E_b/N_o >\sim 10$, where E_b is the energy per bit and $N_o = kT$ is the *noise power density* [W Hz^{-1}] = [J]. A bit is a single yes-no piece of information. Boltzmann's constant $k \cong 1.38\times 10^{-23}$ [J $^oK^{-1}$], and T is the *system noise temperature*, which might approximate 100K in a good system at RF frequencies. Thus the minimum energy required to detect each bit of information is $\sim 10N_o = 10\ kT \cong 10^{-20}$ [J].

An alternative to such observations of MEMS sensor voltage transients is to observe changes in resonant frequency of an LC resonator that includes the sensor capacitance; this approach can reduce the effects of low-frequency interference.

6.6.2 Magnetic MEMS sensors

Microscopic magnetic sensors are less common than electrostatic ones because of the difficulty of providing strong inexpensive reliable magnetic fields at microscopic scales. High magnetic fields require high currents or strong permanent magnets. If such fields are present, however, mechanical motion of a probe wire or cantilever across the magnetic field lines could produce fluctuating voltages, as given by (6.1.4).

6.6.3 Hall effect sensors

Hall effect sensors are semiconductor devices that produce an output voltage V_{Hall} proportional to magnetic field $\overline{H}$, where the voltage is produced as a result of magnetic forces on charge carriers moving at velocity $\overline{v}$ within the semiconductor. They can measure magnetic fields or, if the magnetic field is known, can determine the average velocity and type (hole or electron) of the charge carriers conveying current. A typical configuration appears in Figure 6.6.2, for which the Hall-effect voltage V_{Hall} is proportional to the current I and to the perpendicular magnetic field $\overline{H}$.

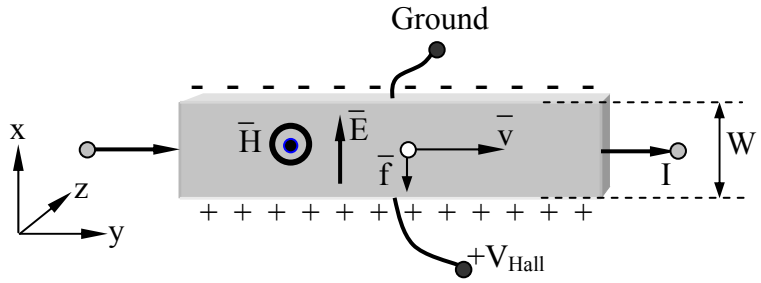

Figure 6.6.2 Hall effect sensor.

The operation of a Hall-effect sensor follows directly from the Lorentz force law:

$$\overline{f} = q\left(\overline{E} + \overline{v} \times \mu_o \overline{H}\right) \quad \text{[Newtons]} \tag{6.6.3}$$

Positively charged carriers moving at velocity $\overline{v}$ would be forced downward by $\overline{f}$, as shown in the figure, where they would accumulate until the resulting electric field $\overline{E}$ provided a sufficiently strong balancing force qE in the opposite direction to produce equilibrium. In equilibrium the net force and the right-hand side of (6.6.3) must be zero, so $\overline{E} = -\overline{v} \times \mu_o \overline{H}$ and the resulting V_{Hall} is:

$$V_{Hall} = \hat{x} \bullet \overline{E} W = v \mu_o H W \quad [V] \tag{6.6.4}$$

For charge carrier velocities of 30 m s^{-1} and fields $\mu_o H$ of 0.1 Tesla, V_{Hall} would be 3 millivolts across a width W of one millimeter, which is easily detected.

If the charge carriers are electrons so $q < 0$, then the sign of the Hall voltage is reversed. Since the voltage depends on the velocity v of the carriers rather than on their number, their average number density N [m^{-1}] can be determined using I = Nqv. That is, for positive carriers:

$$v = V_H / W\mu_o H \left[ms^{-1}\right] \tag{6.6.5}$$

$$N = I/qv \tag{6.6.6}$$

Thus the Hall effect is useful for understanding carrier behavior (N,v) as a function of semiconductor composition.

6.013 Electromagnetics and Applications
Spring 2009